The effect of halogen on the structural, optoelectronic, and luminescent properties of hybrid (1,5-Pentanediamine)PbX_4 (X=Cl, Br, I) perovskites

D.S. Shtarev[1,2a,*], M.I. Balanov[2,b], A.Ju. Major[2,3,c], A.V. Gerasimenko[4,d], R. Kevorkyants[5,e], D.A. Zharovov[5,f], K.M. Bulanin[6,g], D.V. Pankin[6,7,h], A.V. Rudakova[6,i], D.A. Chaplygina[2,j], N.I. Selivanov[5,k], A.V. Emeline[5,l]

[1] Department of Materials Science, Shenzhen MSU-BIT University, PRC.
[2] Institute of High Technologies and Advanced Materials of the Far Eastern Federal University, Vladivostok, Russky Island, Ajax, 10, 690022, Russian Federation.
[3] Institute of Automation and Control Processes, Far Eastern Branch, Russian Academy of Sciences, Russian Federation.
[4] Institute of Chemistry, Far Eastern Branch, Russian Academy of Sciences, Russian Federation.
[5] Saint-Petersburg State University, Laboratory 'Photoactive Nanocomposite Materials', Russian Federation.
[6] Saint-Petersburg State University, Laboratory 'Photonics of Crystals', Russian Federation.
[7] Saint-Petersburg State University, Center for Optical and Laser Materials Research, Russian Federation.

[a] shtarev@mail.ru, [b] balanov.mi@dvfu.ru, [c] mayor@iacp.dvo.ru, [d] gerasimenko@ich.dvo.ru,
[e] ruslan.kevorkyants@gmail.com, [f] dmzharovov@gmail.com, [g] k.bulanin@spbu.ru,
[h] dmitrii.pankin@spbu.ru, [i] aida.rudakova@spbu.ru, [j] chaplygina.dal@dvfu.ru,
[k] selivanov_chem@mail.ru, [l] alexei.emeline@spbu.ru
* - Corresponding author (ORCID: 0000-0002-1274-0183)

Supplementary materials

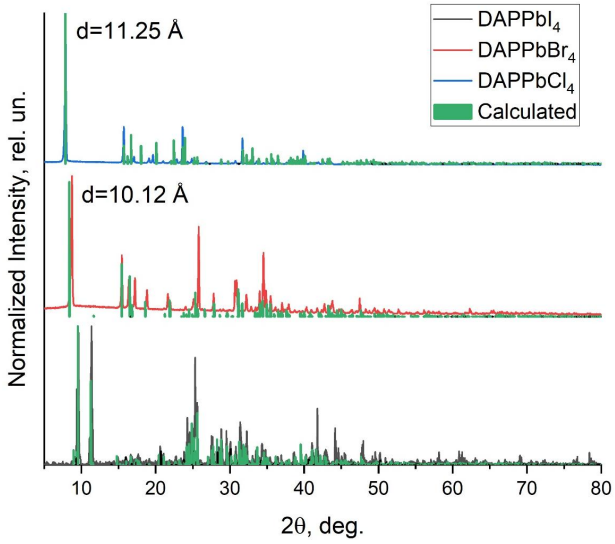

Figure S1. Powder XRD spectra of $DAPPbX_4$, (X = Cl, Br, I) and the reference XRD spectrum of $DAPPbI_4$.

Table S1. Selected crystal and refinement data for $DAPPbX_4$, (X = Cl, Br).

	$DAPPbCl_4$	$DAPPbBr_4$
Formula	$NH_3(CH_2)_5NH_3PbCl_4$	$NH_3(CH_2)_5NH_3PbBr_4$
Formula weight	453.19	631.03
Temperature, K	100(2)	150(2)
Radiation type	Mo Kα	Mo *Kα*
Space group	C2221	C2/c
Shape / size, mm	Prism / 0.037 □ 0.13 □ 0.16	Prism / 0.15□0.20□0.24
a, Å	7.4322(6)	21.4488(11)
b, Å	8.0456(6)	8.1241(4)
c, Å	22.5432(18)	8.2662(4)
β, °		100.820(3)
V, Å / Formulae unit	1348.00(18) / 4	1414.80(12) / 4
D_{calc} (g/cm^3) / μ (mm^{-1})	2.233 / 13.270	2.963 / 23.185
□*θ* range (°)	3.62 – 28.50	1.933 – 26.086
Range of *h*, *k* and *l*	–6/9, –10/10, –30/30	–26/26, –10/10, –10/10
F(000)	840	1128
Refl. [meas./uniq./*I*>2σ(*I*)]	6297/1718/1700 (Rint = 0.0211)	23026/1409/1243 (R_{int} = 0.0478)
Number of parameters	108	108
GooF	1.068	1.142
R_1, wR_2 [$F^2 > 2\sigma(F^2)$]	0.0176, 0.0437	0.0231, 0.0540
R_1, wR_2 (all data)	0.0179, 0.0439	0.0294, 0.0560
$\Delta\rho_{min}$, $\Delta\rho_{max}$ (e/Å^3)	–0.469, 4.515	a–1.047, 1.894
Deposit number CCDC	2269541	2269539

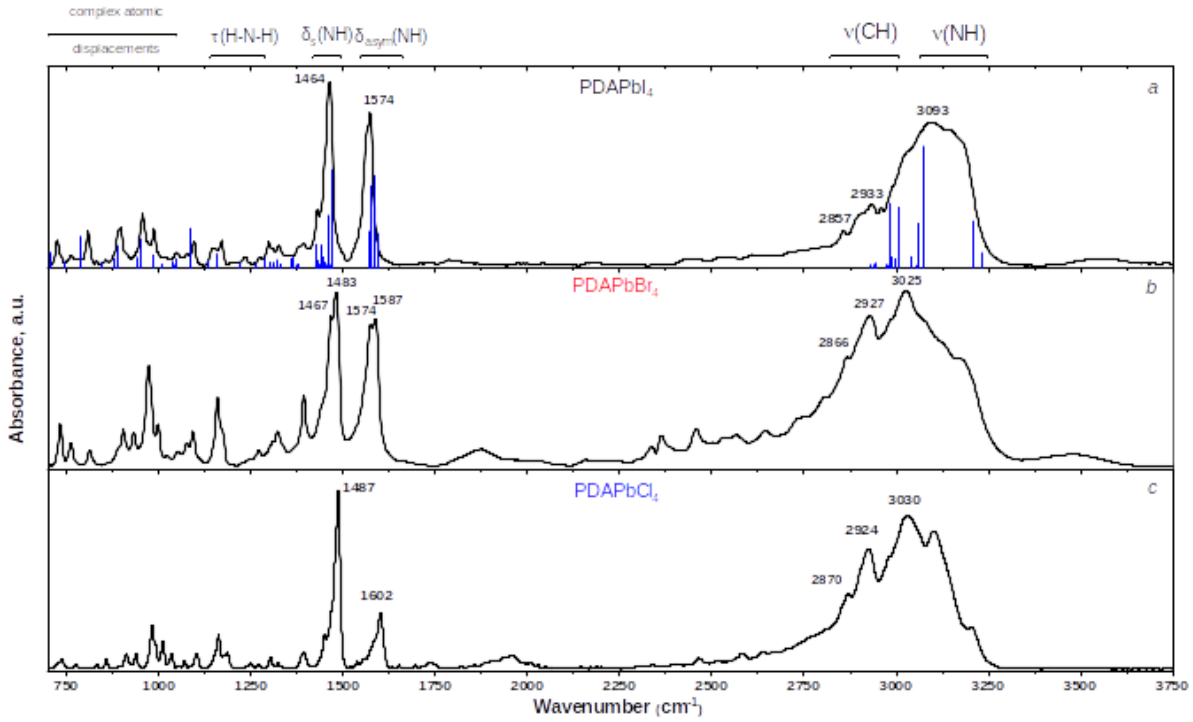

Figure S2. FTIR spectra of *a* – $PDAPbI_4$, *b* – $PDAPbBr_4$, *c* – $PDAPbCl_4$. The calculated IR spectrum of $PDAPbI_4$ is represented by the blue bars.

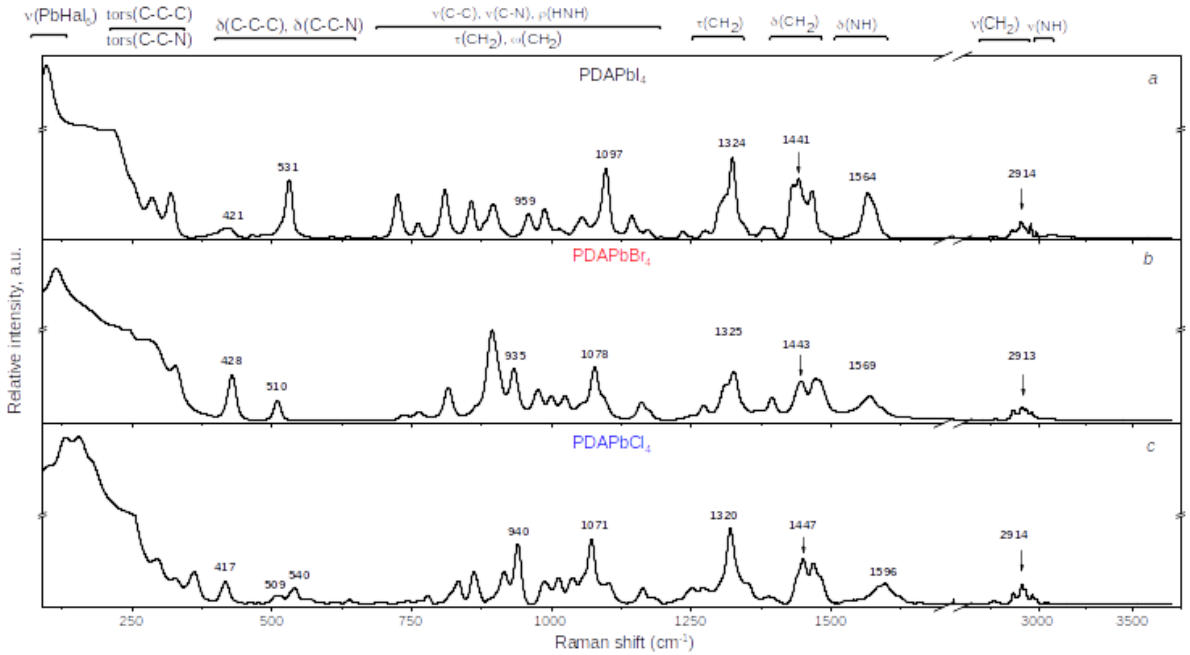

Figure S3. Raman spectra of *a* – $PDAPbI_4$, *b* – $PDAPbBr_4$, *c* – $PDAPbCl_4$.

Table S2. Frequencies and assignment of the selected characteristic Raman and IR peaks in the range [95-1600] cm^{-1}.

$PDAPbCl_4$		$PDAPbBr_4$		$PDAPbI_4$			Assignment
Raman	FTIR	Raman	FTIR	Raman	FTIR	FTIR (calculated)	
1596	1602	1592	1587	1573	1574	1584	δ_{asym}(H-N-H)
1587	1585	1569	1575	1564	1565	1576	δ_{asym}(H-N-H)
1482	1487	1487	1483	1466	1464	1471	δ_s(H-N-H)
1467	1468	1475	1467	1444	1448	1461 1465	predominantly δ_s(H-N-H) ν(C-N)
1447	1450	1443	1444	1441	1431	1425,	δ(H-C-H)

$PDAPbCl_4$		$PDAPbBr_4$		$PDAPbI_4$			Assignment
Raman	FTIR	Raman	FTIR	Raman	FTIR	FTIR (calculated)	
						1440	
1320	n/o	1325	1324	1324	1326	1322	predominantly $\tau(CH_2)$
1071	1071	1078	1076	1097	1097	1087	ν(C-C) ν(C-N) ρ(HNH) $\omega(CH_2)$ $\tau(CH_2)$
1037	1036	1024	1024	1015	1015	1011	complex atomic displacements ν(C-C) ρ(HNH) $\tau(CH_2)$ ν(C-N)
1012	1012	974	974	986	986	984	complex atomic displacements ν(C-C) ν(C-N), ω(HNH), ω(HCH), ρ(HNH)
940	982	935	933	959	957	952	complex atomic displacements ν(C-C)

$PDAPbCl_4$		$PDAPbBr_4$		$PDAPbI_4$			Assignment
Raman	FTIR	Raman	FTIR	Raman	FTIR	FTIR (calculated)	
							ν(C-N), $\tau(CH_2)$ ρ(HNH) τ(HNH)
833	832	893	n/o	857	857	847	complex atomic displacements ν(C-C) ν(C-N) $\rho(CH_2)$ ρ(HNH)
509 540		510		531			predominantly δ(CCC) ρ(HNH)
417		428		421			predominantly δ(NCC)
327		330		320			tors(HNCC) δ(NCC) tors(HCCC)
297		289		286			tors(HNCC)
98 132 156 178		91 112		98			lattice modes

* The ν, δ, ρ, w, and τ notations denote stretching, bending (scissoring), rocking, wagging, and twisting vibrations, respectively.

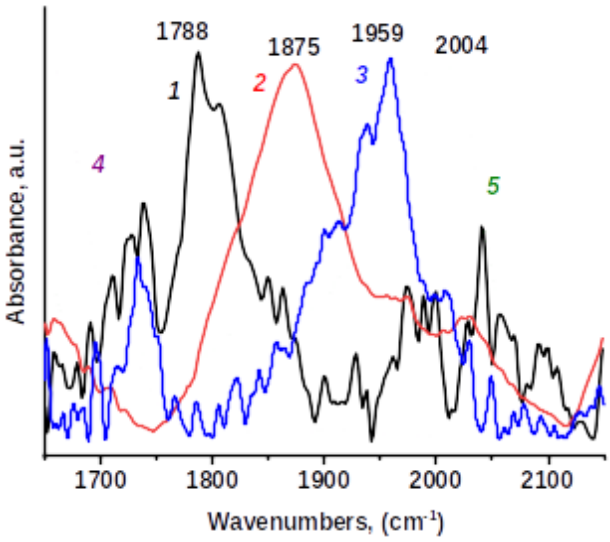

Figure S4. Normalized FTIR spectra in the range of (tor(C-C-N)+$_{as}$(NH)) combination band: 1 – $PDAPbI_4$, 2 – $PDAPbBr_4$, 3 – $PDAPbCl_4$. Spectra of solid PDA (*4)* and PDA dihydrochloride (*5*) diluted in KBr pellets are presented for comparison [32].

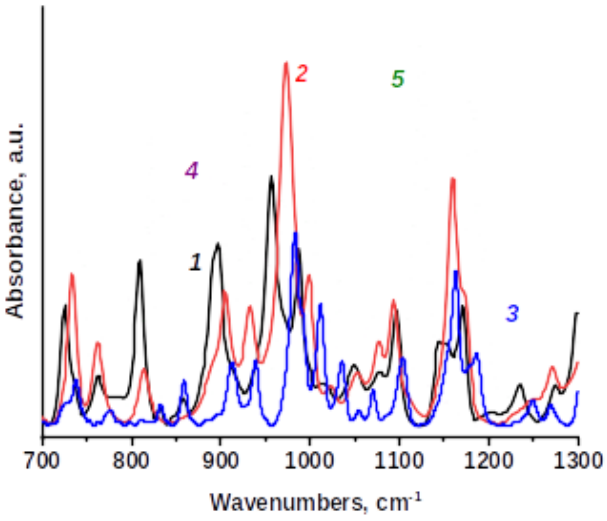

Figure S5. Normalized FTIR spectra in (NH) frequency range: 1 – $PDAPbI_4$, 2 – $PDAPbBr_4$, 3 – $PDAPbCl_4$. Spectra of solid PDA (*4)* and PDA dihydrochloride (*5*) diluted in KBr pellets are presented for comparison [32].

Luminescence lifetimes of the synthesized perovskites were determined using the setup in Figure S6. Working characteristics of the laser excitation source YAG laser Q-Smart 850 (Quantel, France): pulse repetition frequency was set to 10 Hz (minimal possible value); pulse energy at 355 nm – ≤ 230 mJ, pulse energy at 266 nm - ≤ 100 mJ; pulse duration 5 ns. The vacuumized sample was placed in the optical nitrogen cryostat LN-121-SPECTR (Cryotrade engineering, Russia). To record the time dependence of the luminescence intensity, a spectrometer was used as part of the spectrograph SP2500 (Princeton Instruments, USA) and CCD-camera with stroboscopic brightness enhancement and time delay generator (minimal exposition 0.1 ns) PicoStar HR (LaVision GmbH, Germany).

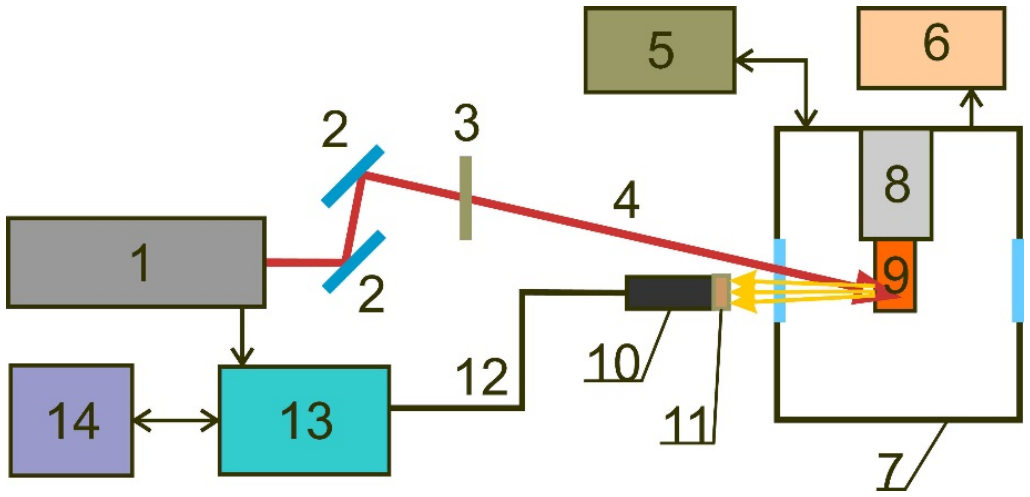

Figure S6. Experimental setup for luminescence spectra recording: 1 — Laser; 2 – Mirror; 3 – Filter UFS-1; 4 – Laser beam; 5 – Thermoregulator; 6 — Vacuum pump; 7 – Cryostat; 8 – Liquid nitrogen; 9 – Sample; 10 – Receiving collimator; 11 – Laser radiation suppression filter; 12 – Optical fiber; 13 – Spectrometer; 14 – Computer.

The studied luminescence was collected using a quartz collimator UV-74 (Ocean Optics, США) and then transmitted via optical fiber into the receiver. Both, the laser excitation and luminescence feedback have used the same cryostat window, therefore, to prevent the reflected laser beam entering the collimator aperture the laser beam and collimator optical axis were shifted and tilted away from the window central normal by 10° – the laser beam - vertically, the collimator axis -

horizontally. To suppress the scattered laser radiation a filter was setup in front of the collimator: in the case of 266 nm light – a glass filter БС-4 (analogous to Schott N-WG295, Germany), in the case of 355 nm – a dichroic filter LP02-355RU-25 (Semrock, USA). The remnant second harmonics laser radiation (532 nm) was suppressed by means of the filter УФС-1 (analogous to Schott UG-1, Germany).

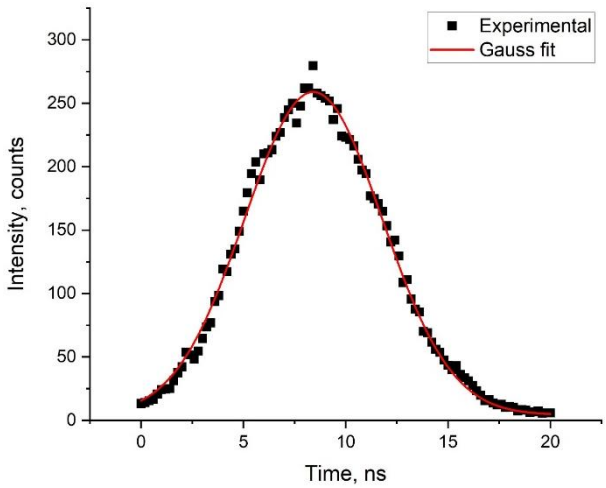

Figure S7. Profile of increasing and decreasing laser pulse intensity for luminescence excitation.